with experiment. However, this agreement can only be fortuitous. The value $\sigma^p \approx -500$ ppm for $V(CO)_6^-$ appears to be too small. The absolute shielding for ^{51}V is not yet known although there are two estimates of σ^p for $^{51}V(CO)_6^-$: -5800 ppm (Juranic[18]) and -5993 ppm (Nakano[28]).[29]

There are two important conditions that are not fulfilled in the region of extrapolation. While $(\partial\sigma/\partial r)_e$ may be dominated by $(\partial\sigma^p/\partial r)_e$ when σ^p is a large negative contribution, this is not likely to hold when $\sigma^p \sim 0$. While the observed $d\sigma/dT$ in solution may be dominated by $d\sigma_0/dT$ when the latter is large compared to intermolecular effects $\sigma_1'(d\rho_{liq}/dT)$, this is not likely to hold in the vicinity of $d\sigma_0/dT \sim 0$. While the empirical correlation in Figure 2 is deceptively linear, as the electrostatic model predicts, the empirical correlation observed for ^{19}F in fluoromethanes is decidedly curved, approaching $d\sigma_0/dT = 0$ asymptotically with F in CH_3F molecule at that extreme end ($\sigma^p \sim 0$).[6] Although all observations indicate that $(\partial\sigma/\partial r)$ and σ^p are related, the true relationship cannot be as simple as the strict proportionality between $(\partial\sigma/\partial r)$ and σ^p which results from the assumptions of the electrostatic model for shielding.

Conclusions

The magnitude of the temperature coefficients of the chemical shifts are much larger for transition metal nuclei than for others (^{19}F, ^{15}N, ^{13}C, ^{31}P). Thus, the effects of intermolecular interactions, while not small in the absolute sense, are small enough to be neglected compared to the total temperature coefficient. Therefore, for transition metal nuclei it is possible to obtain the effects of rovibrational averaging on nuclear shielding in complexes in solution, without zero-pressure limit gas-phase studies.

We have presented a theory which accounts for the observed temperature coefficients of nuclear shielding for transition metal nuclei in complexes in solution and the relatively large isotope shifts which are induced by substitution of ligand atoms. As typical examples, the vibrational analysis of $V(CO)_6^-$ and $Co(CN)_6^{3-}$ provide dynamic averages of the bond displacements V-C, C-O, Co-C, and C-N, in terms of anharmonic force constants, taking into account Morse stretching anharmonicity as well as nonbonded interactions. These dynamic averages are temperature and mass dependent in a way which successfully accounts for the observed NMR shifts with temperature and isotopic substitution in these complexes. The conclusions for these two typical cases provide a general explanation for temperature coefficients and isotope shifts of transition metal nuclei in their complexes.

We have observed a correlation between the temperature coefficients and the chemical shifts. This correlation is qualitatively consistent with the simple electrostatic model for shielding which was originally proposed in the 1960s and recently refined by Bramley et al. While the electrostatic model for shielding is very successful in correlating chemical shifts of a wide variety of transition metal complexes and also in correlating the temperature coefficients of the chemical shifts with the chemical shifts themselves, the exact form of the predicted dependence of transition metal shielding on the metal-ligand distance is probably incorrect.

Acknowledgment. This research was supported in part by the National Science Foundation (CHE85-05725) and the Fonds der Chemischen Industrie, F.R.G.

(28) Nakano, T. *Bull. Chem. Soc. Jpn.* **1977**, *50*, 661-665.

(29) These estimates are not independent since both values are based on Nakano's value for VO_4^-. The latter method gives σ^p values for Mn in $Mn(CO)_5X$ that are considerably different from the ab initio calculations, so the ^{51}V estimates may be seriously flawed.

Benzobisdithiazole (BBDT): An Electron Spin Resonance Study

Elmar Dormann,*† Michael J. Nowak, Keith A. Williams, Richard O. Angus, Jr., and Fred Wudl*

Contribution from the Institute for Polymers and Organic Solids, Department of Physics, University of California, Santa Barbara, California 93106. *Received July 7, 1986*

Abstract: We report on ESR properties of the title compound in different oxidation states in solution and in the solid state. Comparative studies of the ESR properties of the deuterated derivatives of BBDT and benzodithiazole (BDT) in conjunction with extended Hückel molecular orbital calculations are also reported. It is shown that BBDT forms a diradical which exists as an oligomer in solution and in the solid state. The radical cation exhibits the expected hyperfine spectrum whereas the diradical does not; explanations for these observations are presented.

In a recent paper we described preliminary findings on our research on the novel title compound[1] which was prepared as part of a program to design molecules which would be stable, neutral diradicals[2] with the intent to generate neutral organic metals. However, we also realized that these molecules may fit a variant along the lines of the McConnell hypothesis where we let the neutral donor be the triplet and the acceptor be the *radical ion derived from the donor*. This modification would allow us to generate homomolecular stacks which could give rise to *ferromagnetic organic metals* (FOM). The McConnell-Breslow and our approaches are sketched in Figure 1.

As can be seen from the figure, our FOM (Figure 1d) has two important differences from one version of the McConnell idea (Figure 1b): (a) the stoichiometry is D_2A (A = monovalent, closed-shell counteranion), rather than simple charge-transfer complex "DA", and (b) degeneracy; i.e., the species on the left of the double-headed arrow are identical with those on the right (a dictate of the spin conservation rules and a consequence of point a). The proposed FOM evolved naturally from extensive research on organic metals and superconductors[3,4] [e.g., $(TMTSF)_2X$]. The crux of our FOM is the design of a stable donor diradical which should have a triplet ground state and should not have a driving force toward dimerization (polymerization). We concluded that the functional group best suited to fulfill these requirements would

† Visiting Scientist from the Physikalisches Institut und Bayreuther Institut für Makromolekül-Forschung (BIMF), Universität Bayreuth, POB 10 12 51, D-8580 Bayreuth, Federal Republic of Germany.

(1) Williams, K. A.; Nowak, M. J.; Dormann, E.; Wudl, F. *Synth. Met.* **1986**, *14*, 233. See also: Wolmershäuser, G.; Schnauber, M.; Wilhelm, T.; Sutcliffe, L. H. *Ibid.* **1986**, *14*, 239.

(2) Wudl, F. *Pure Appl. Chem.* **1982**, *54*, 1051.

(3) Bechgaard, K.; Jerome, D. *Sci. Am.* **1982**, *247*, 52.

(4) Wudl, F. *Acc. Chem. Res.* **1984**, *17*, 227 and references therein.

0002-7863/87/1509-2594$01.50/0

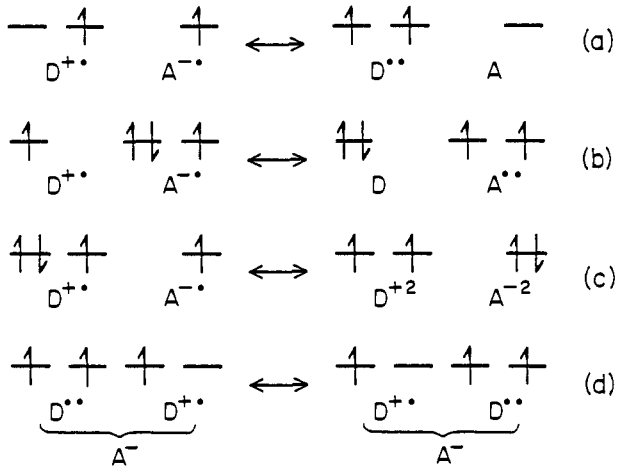

Figure 1. (a and b) The McConnell model as applied to a heteromolecular stack consisting of donors (D) and acceptors (A), where the neutral donor or acceptor is a triplet diradical. (c) The Breslow approach to organic ferromagnets, where the redox potentials of the donor-derived monocation and acceptor-derived monoanion are carefully matched. (d) The stack of an FOM consisting of donors with ground-state triplets and radical cations derived from the same donors plus closed-shell counteranions (A^-) at a nearby site in the lattice.

be the [-S-N-S-]• group as evidenced from the lack of crosslinking in $(SN)_x$.[5]

It is clear from the above that it was imperative that we learn as much as possible about the magnetic properties of the BBDT molecule in solution. Important parameters to be established were the strength of the exchange interaction between the unpaired electrons in **1a** and the nature of the interaction: ferromagnetic or antiferromagnetic (triplet or singlet). We also sought information regarding the molecule's tendency toward dimerization (or oligomerization). We believed that the latter could be gleaned from a combination of electron spin resonance spectroscopy and quantum mechanical molecular orbital calculations.

In this paper we report a detailed study of the electron spin resonance (ESR) properties in solution and in the solid state of the new "donor" molecule, BBDT (**1**) in two of its three stable oxidation states [neutral (**1a**) and radical cation (**1b**)], as well as a comparison of these with spectroscopic properties of benzodithiazole (BDT, **2**) and the deuterated derivatives (**1c** and **1d**).

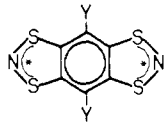

1

1a: *,* = •,•; Y = H 1c: *,* = •,•; Y = D
1b: *,* = •,+; Y = H 1d: *,* = •,+; Y = D

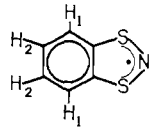

2

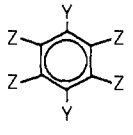

3a: Y = H, Z = SCH_3
3b: Y = D, Z = SCH_3

3

(5) Haddon, R. C.; Wasserman, S. R.; Wudl, F.; Williams, G. R. J. *J. Am. Chem. Soc.* **1980**, *102*, 6687.

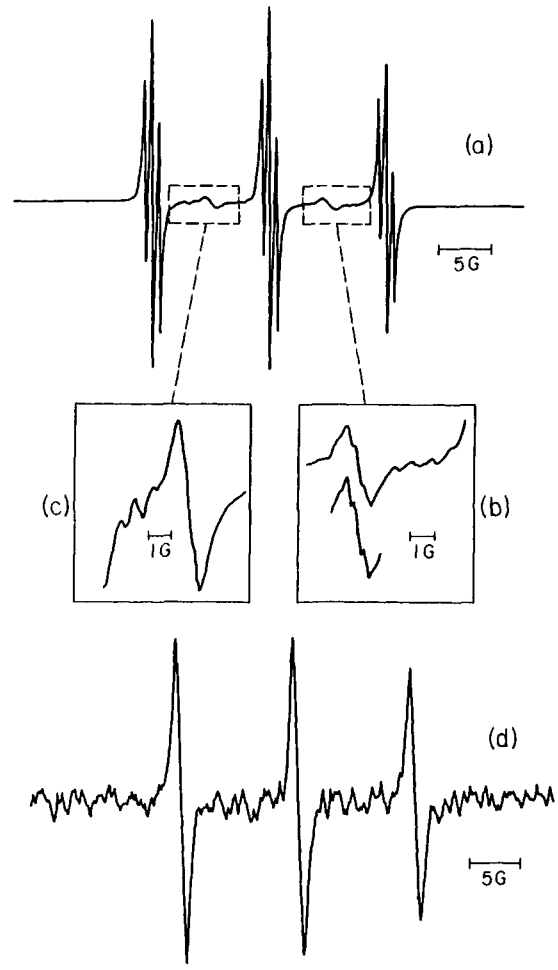

Figure 2. ESR spectrum of benzobisdithiazole in dilute solution at room temperature (microwave frequency 9.3 GHz, modulation frequency 12.5 kHz; b, 100 kHz). (a) **1a** in CH_2Cl_2 (6×10^{-3} M), (b) blown-up section of (a) (modulation amplitude 0.332/0.12 G_{pp}), (c) blown-up section of (a) for a more concentrated solution (2×10^{-2} M), (d) **1c** in $CDCl_3$ (10^{-3} M).

We also report on the correlation of these results with MO calculations. Finally, to obtain a more complete picture of the magnetic properties of a tetrathio-substituted benzene, we studied the radical cation derived from a synthetic precursor to **1**, the tetrathiomethyl compound **3**.

Results and Discussion

1. Electron Spin Resonance Spectroscopy of the BBDT Diradical and Related Molecules. The ESR spectrum of the BBDT diradical (**1a**) in dilute dichloromethane solution was recorded with help of an IBM Instruments (Bruker) E-200 D ESR spectrometer (9.3 GHz). The spectrum (as shown in Figure 2a) consists mainly of a triplet of triplets (*tot*). We observed also two weaker lines (*wq*) centered between the *tot* lines, whose relative intensity varied from sample to sample (Figure 2b). For sufficiently concentrated solutions, a very weak doublet of triplets (*dot*) could also be resolved (Figure 2c).

The wide triplet splitting is due to the interaction of the radical electron spin with one nitrogen nucleus (^{14}N, $I = 1$) giving rise to a 1:1:1 intensity ratio as is observed within the error limit. The radical electron also interacts with two equivalent protons; this leads to the triplet structure of each line of the triplet. The integrated ESR line could reasonably be decomposed into the corresponding 1:2:1 intensity pattern. This spectrum can be described with the following parameters of the standard spin-Hamiltonian of an isotropic average in the liquid:

$$g = 2.0063 \pm 0.0002$$

$$a(^{14}N) = (11.24 \pm 0.04)\ G$$

$$a(H) = (0.68 \pm 0.04)\ G$$

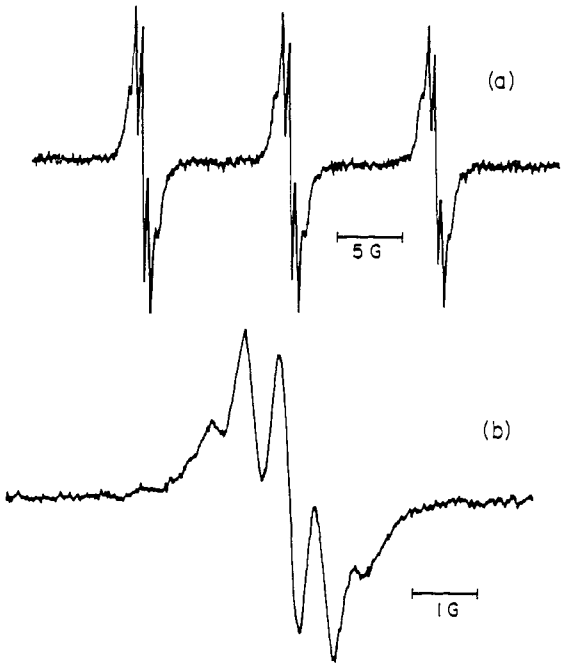

Figure 3. ESR spectrum (a) and blown-up section thereof (low-field line) (b) of benzodithiazole (**2**) in dilute solution of $CDCl_3$ at room temperature (9.3 GHz, modulation frequency 12.5 kHz).

when a spin quantum number $S = {}^1/_2$ is used as would be appropriate for a *single* radical. At first sight, this analysis seems to be in contradiction with the picture of a *di*radical (**1a**). It is, however, as we will show in the following, in agreement with the explanation that the *tot* ESR signal, shown in Figure 2a, originates from dimers or longer oligomers of **1a**. The two spins $S = {}^1/_2$ of those oligomers are separated far enough to render exchange interaction negligible.

The *dot* lines, whose overall intensity is about 3.5×10^{-3} that of the *tot*'s intensity (cf. Figure 2a and expansion in Figure 2c), stem from the same kind of radical electrons interacting with ^{15}N ($I = {}^1/_2$) instead of ^{14}N; ^{15}N occurs to about 0.36% in the natural isotopic mixture. We derived:

$$a(^{15}N) = (15.67 \pm 0.11)\ G$$

all other parameters being unchanged. The ratio of $a(^{15}N)$ to $a(^{14}N)$ observed is in perfect agreement with that of the nuclei's gyromagnetic ratios.

The observation of the well-*resolved proton hyperfine splitting* for BBDT was at first sight surprising, since such splitting was reported to be observable only with difficulty for BDT (**2**).[6] Therefore, we reanalyzed the ESR spectrum of BDT in dilute solution. For a dilute solution of BDT in dichloromethane, an ESR spectrum was observed consisting of a triplet, very similar to the spectrum shown in Figure 2d, with

$$g = 2.0067 \pm 0.0002$$

$$a(^{14}N) = (11.16 \pm 0.02)\ G$$

and about 1.5 G_{pp} line width for each component, in qualitative agreement with the data reported before.[6] We observed that the BDT radical is relatively unstable. An ESR spectrum could, however, be resurrected by light even under conditions which normally gave a poor spectrum. Reanalysis of the ESR spectrum of BDT in a carefully treated dilute solution in deuteriochloroform resulted in the much better resolved spectrum reported in Figure 3a; one component of the spectrum is shown on an extended scale in Figure 3b. Inspection of the integrated spectrum revealed that each triplet component consists of a quintet with about 1:4:6:4:1 intensity ratio. This shows that the two sets of protons of BDT are almost equivalent. We derive

$$\bar{a}(H) = (0.51 \pm 0.07)\ G$$

From the differences of the different components' widths, we can estimate that

$$|a(H_1) - a(H_2)| \leq 0.06\ G$$

Using McConnell's relation[7]

$$a(H) = Q\rho_C \text{ with } Q = -23\ G$$

we conclude that the BDT radical's electron has about 2% of its density on each of the four H-bearing carbons of the ring. This compares favorably with the value of about 3% that can be estimated for the two H-bearing carbons of BBDT.

For further comparison, we also analyzed the ESR spectra of the radical cations **3a** and **3b**[8] in dilute solution in H_2SO_4, represented in Figures 4a and 4b. Again, we found about 3% spin density on the H-bearing ring carbons [spin-Hamiltonian parameters: $g = 2.0075 \pm 0.0002$, $a_{CH}(H) = (0.70 \pm 0.03)$ G, $a_{CH_3}(H) = (2.55 \pm 0.03)$ G].

As a final proof of our conclusion, that the triplet structure of the *tot* and *dot* lines of BBDT is due to the interaction with two equivalent protons and not one second ^{14}N (1:1:1) with weaker isotropic coupling, we prepared also the deuterated molecule (**1c**). Because of the small deuteron hyperfine coupling constant of 0.1 G, the corresponding quintet line structure was not resolved. Instead a pure triplet

$$a(^{14}N) = (11.22 \pm 0.01)\ G$$

with line widths as low as 0.6 G_{pp} was observed (Figure 2d) in full support of our earlier analysis.

Comparison of the ESR spectrum of the BBDT diradical given in Figure 2a with the ESR spectra of radical pairs occurring in

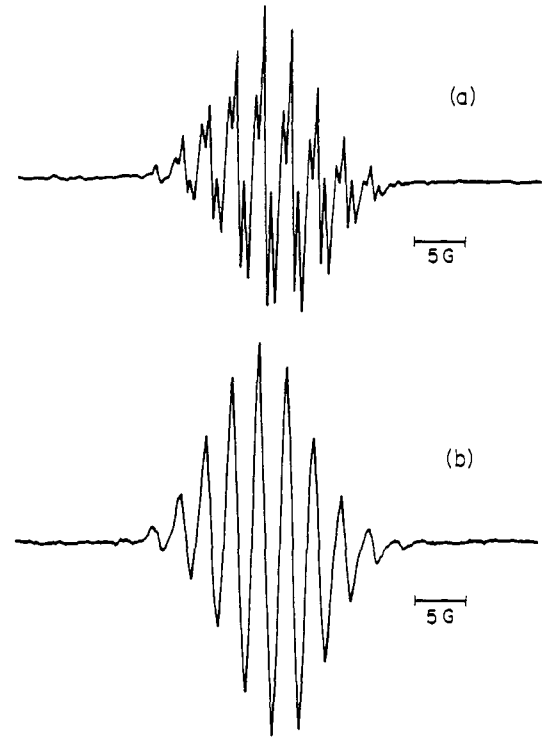

Figure 4. ESR spectrum of tetrakis(methylthio)benzene)$^{\bullet+}$ in dilute solution of concentrated H_2SO_4 at room temperature (9.4 GHz): (a) **3a** (100-kHz modulation frequency), (b) **3b** (12.5-kHz modulation frequency).

(6) Wolmershäuser, G.; Schnauber, M.; Wilhelm, Th. *J. Chem. Soc., Chem. Commun.* **1984**, 573.

(7) Box, H. C. *Radiation Effects: ESR and ENDOR Analysis*; Academic Press: New York, 1977.

(8) Alberti, A.; Pedulli, G. F.; Tiecco, M.; Testaferri, L.; Tingoli, M. *J. Chem. Soc., Perkin Trans. 2* **1984**, 975.

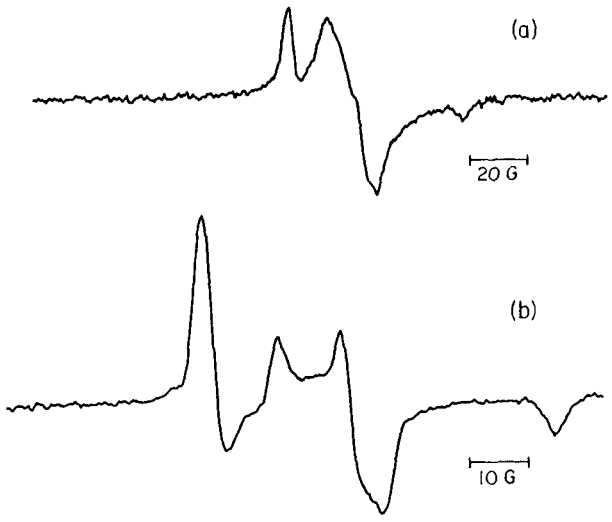

Figure 5. ESR of frozen solution ($\sim 10^{-2}$ M) of benzobisdithiazole at 100 K (9.35 GHz, 12.5-kHz modulation frequency): (a) **1a** in dichloromethane, (b) **1a** in 2-methyltetrahydrofuran.

spin-labeling experiments, especially of biradicals due to double labeling with nitroxide radicals, showed striking similarities between both.[9] Employing the techniques established in this field of magnetic resonance, we also analyzed ESR spectra of glassy frozen solutions of **1a** and **1c** in order to get information on the anisotropy of g and hyperfine tensors as well as on the separation of the diradical spins. Figure 5a shows the spectrum of BBDT in CH_2Cl_2 frozen glass and Figure 5b in MeTHF frozen glass, both at about 100 K. Along the lines established by others[9,10] and using DPPH as g standard, $A_{zz}(^{14}N) = +(29.7 \pm 0.1)$ G and $g_z = 2.0025 \pm 0.0003$ could be derived from the high- and low-field singularities. From these quantities, we can calculate:

$$\bar{A}_\perp = \tfrac{1}{2}(A_{xx} + A_{yy}) = \tfrac{1}{2}(3a - A_{zz}) = +(2.0 \pm 0.1) \text{ G}$$

$$\bar{g}_\perp = \tfrac{1}{2}(g_{xx} + g_{yy}) = \tfrac{1}{2}(3g_{iso} - g_z) = 2.0082 \pm 0.0003$$

The anisotropy of A and g tensors agree qualitatively with that derived for axially symmetric nitroxide spin labels.[11] The derived values fall between those reported for dithiazolidin-2-yl and dithiazol-2-yl radicals.[10] Using

$$a(^{14}N) = Q_{N,s}\rho_{N,s} \text{ with } Q_{N,s} = +549.5 \text{ G}$$

$$A_{\parallel,p}(^{14}N) = A_{zz} - a = Q_{N,p}\rho_{N,p} \text{ with } Q_{N,p} = +34.1 \text{ G (cf. ref 7)}$$

we estimate that 54% of the radical electron spin residues on the nitrogen p orbital and only 2% on the nitrogen s orbital. Remember that 3% of the spin density was observed at each of the two H-bearing ring carbons; thus, only 38% is left for the sum of the remaining four ring carbons and the sulfur atoms. The absolute value and anisotropy of the g factor is in keeping with this picture.

In a single crystal with well-oriented BBDT molecules, we could have observed the angular dependence of the ESR lines and thus have determined the zero-field splitting (and also the dipolar interaction between both $S = {}^1/_2$ radical electron spins[7]) of the $S = 1$ (triplet) state. Under these conditions, the exchange-coupled diradicals would be ferromagnetic and thus the triplet state would be the ground state, or the exchange-coupled diradicals would be weakly antiferromagnetic such that the $S = 1$ excited state would lie close enough above the $S = 0$ (singlet) ground state to have a reasonable thermal population. It is well known, however, that dipolar interaction between both coupled spins can also be derived from the broadening of the powder pattern in glassy frozen solution,[9] assuming point dipoles of the extrema of the broadening amount to[7]

$$\Delta B = 3g\mu_B/r^3$$

From the broadening of about 64 G in the integrated spectrum of Figure 5a, we derived 9.5 Å as the minimal separation of the magnetic point dipoles. This indicates that the diradicals observed here are at least dimers of **1a**. From the peak widths in Figure 5b and the overall broadening in an integrated version of this spectrum, we derived shortest point dipole separations between 24.7 and 16.5 Å. This indicates that in this sample a considerable part of the diradicals observed must originate from trimers or even longer oligomers.

Further evidence for the tendency of BBDT (**1a**) to dimerize (or oligomerize) was observed from several other experiments. (1) Absolute calibration of the ESR signal strength with an NBS ruby standard indicated that, at room temperature in dilute dichloromethane solution, at best only 1% of the expected number of spins was observed when all BBDT molecules would carry their two $S = {}^1/_2$ spins. This signal intensity loss was not due to the observation of the ESR signal of an excited triplet state, because the signal intensity followed a Curie law: at 100 K compared with room temperature, the ESR intensity (Figure 2a to Figure 5a) increased within a factor (0.77 ± 0.31) as strongly as expected from a Curie law behavior, allowing at best for a value of 100 K for the separation of an excited triplet state from a ground-state singlet and thus a reduction of the signal intensity to 68% at room temperature, not to 1% as observed. In contrast, the tendency toward polymerization could explain such a reduction in number of free spins. (2) When solutions of BBDT in dichloromethane were stored for extended periods of time, a precipitate was observed. (3) Since we derived the anisotropy of g and A tensor from the frozen solution before, we were able to determine quantitatively the correlation times of isotropic molecular rotation in dichloromethane solution:

$$\tau_c = \frac{45\sqrt{3}\hbar W(+1)\{1 - [h(+1)/h(-1)]^{1/2}\}}{64\pi\mu_B B_0[A_{zz} - (A_{xx} + A_{yy})/2][g_z - (g_x + g_y)/2]}$$

with $W(+1)$ the peak–peak width of the central line of the low-field triplet and $h(+1)$ ($h(-1)$) the peak height of the low- (high-) field triplet's central component.[10] Figure 2a shows clearly the characteristic asymmetry of the ESR spectrum, which is well known and amply used for nitroxide spin labels,[9-11] with the high-field lines broader and, therefore, of smaller peak-to-peak height in the differentiated spectrum than the low-field lines (for $A_{zz} > A_\perp$ and $g_z < g_\perp$). For different solutions of BBDT in CH_2Cl_2 and without stirring the solutions before the ESR experiment, we observed variation of the rotational correlation time between 2.3 and 7.8×10^{-12} s, indicating a factor of 1.5 difference in third power averaged molecular radius. After an older CH_2Cl_2 solution was stirred, correlation times as long as 22×10^{-12} s were found, indicating a factor of 2.1 in averaged length. (Applying the simple Debye model with

$$\tau_c = (4\pi a^3/3k_BT)\eta$$

spherically averaged molecular radii from 1.74 up to 3.66 Å could be derived, with the upper end being much larger than usually observed with molecules of the monomer's size).

Thus, we conclude that the *tot* ESR spectrum, as well as the *dot* spectrum shown in Figure 2a, is due to dimers and oligomers of BBDT that are long enough to render exchange interaction of the two radical electrons $S = {}^1/_2$ negligible. Usually this is supposed to occur for distances larger than[9] 7–8 Å. The ESR spectrum of these diradicals thus cannot be distinguished from one that would be due to a single unpaired electron. The spin density is largely concentrated on the outer nitrogens. From the ESR analysis alone we cannot decide if a dichloromethane solution contains essentially *no* BBDT *monomers* at all or if there is indeed a large percentage (e.g., up to 98%) with, however, a strongly antiferromagnetically coupled singlet ($S = 0$) ground state and

(9) Likhtenshtein, G. I. *Spin Labeling Methods in Molecular Biology*; Wiley: New York, 1976.
(10) Fairhurst, A. Sh.; Pilkington, R. S.; Sutcliffe, L. H. *J. Chem. Soc., Faraday Trans. 1* **1983**, *79*, 439.
(11) Berliner, L. J. *Spin Labeling II: Theory and Applications*; Academic Press: New York, 1979.

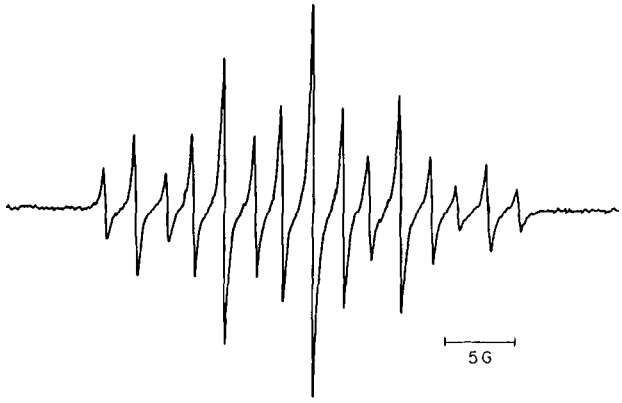

Figure 6. ESR spectrum of benzobisdithiazole radical cation (**1b**) in aqueous solution ($\sim 10^{-2}$ M) at room temperature (9.5 GHz, 100-kHz modulation frequency).

with their $S = 1$ excited triplet state so far above that it is thermally not populated.

We now come to the discussion of the two weaker lines (*wq*) that are centered between the *tot* lines of the BBDT oligomer diradicals. In this respect, again Figure 2a shows striking similarity to ESR spectra of nitroxide double-labeled molecules with direct exchange interaction between the two radical spins.[9] Accordingly, the line shape of Figure 2b, or its integrated version, can reasonably be decomposed into a quintet with 1:4:6:4:1 intensity ratio and a hyperfine coupling constant of

$$a(\mathrm{H}) = (0.35 \pm 0.03)\ \mathrm{G}$$

just half the value of the separated radical spins. This indicates that each electron spin interacts here with all four protons at both sides of the dimer or at both ends of the oligomer. The overall intensity distribution of the complete spectrum shown in Figure 2a is in keeping also with the interpretation that the two *wq* lines are only two out of a quintet of quintets with 1:2:3:2:1 intensity distribution, the middle and outer one's overlapping with the *tot* lines. This would indicate that they originate from an exchange coupled $S = 1$ triplet state with the same g factor and

$$a(^{14}\mathrm{N}) = (5.62 \pm 0.04)\ \mathrm{G}$$

again one-half of the nitrogen coupling constant given above. A priori, it is not clear if these lines originate from ferromagnetically coupled BBDT dimer diradicals or from diradicals of oligomers that are so long that the ends can easily come into close contact, giving rise to a time-dependent (dynamic) exchange interaction. As we mentioned above, the relative intensity of the *wq* lines was sample dependent. It varied between 2 and 7% of that of the *tot* spectrum. We observed that this variation is correlated with the variation of the rotational correlation time τ_c. Samples with larger τ_c and, therefore, in average larger molecules gave larger relative *wq* intensities. We take this as indication that the weak ESR spectrum results from exchange interaction of two radical spins at the ends of longer BBDT oligomers.

2. BBDT Radical Cation in Solution, Glass, and Solid Salt. The ESR spectrum of the BBDT radical cation (**1b**) in aqueous solution is shown in Figure 6. It consists of a quintet of triplets, proving that the radical electron spin is interacting with two equivalent nitrogen nuclei ($I = 1$) and two equivalent protons ($I = {}^1/_2$). The observed intensities are in agreement with the expected 1:2:3:2:1 and 1:2:1 patterns. The high-field lines are again somewhat broader and, therefore, of smaller peak-to-peak height than the low-field lines as a consequence of limited rotational motion speed. We derived ($S = {}^1/_2$):

$$g = 2.0068 \pm 0.0002$$

$$a(^{14}\mathrm{N}) = (6.24 \pm 0.03)\ \mathrm{G}$$

$$a(\mathrm{H}) = (2.20 \pm 0.03)\ \mathrm{G}$$

From one solution that contained radical cation **1b** and diradical **1a** together, we could determine that the g factor of **1b** is larger than that of **1a** by $+(2.5 \pm 0.6) \times 10^{-4}$, in agreement with the larger spin density on nitrogen for **1b** that we found from analysis of a frozen solution, as explained below.

We also analyzed the ESR spectrum of a solution containing BBDT radical cations that were deuterated to at least 85% (**1d**). The spectrum was dominated by a quintet of quintets (2 N, 2 D, $I_D = 1$) with $a(^{14}\mathrm{N}) = (6.24 \pm 0.04)$ G and $a(\mathrm{D}) = (0.335 \pm 0.015)$ G, in perfect agreement with the parameters derived for **1b**. The ESR spectrum also contained a weaker quintet of doublets of triplets (2 N, 1 H, 1 D) and a still weaker quintet of triplets (2 N, 2 H), all with the coupling parameters already derived before.

The ESR spectrum of **1b** in frozen solution was taken in sulfolane at about 100 K. We derived $A_{zz}(^{14}\mathrm{N}) = (16.3 \pm 0.1)$ G and $g_z = 2.0026 \pm 0.0007$. This allowed us to calculate

$$\bar{A}_\perp = {}^1/_2(A_{xx} + A_{yy}) = (1.2 \pm 0.1)\ \mathrm{G}$$

$$\bar{g}_\perp = {}^1/_2(g_x + g_y) = 2.0089 \pm 0.0006$$

The hyperfine coupling constants derived for the radical cation here indicate that its wave function has a distribution that is clearly distinct from that of the diradical: the spin density at the H-bearing ring carbons is much larger (10% on each of them). Since for each of the two nitrogens we find 1% s and 30% p density, also the overall nitrogen spin density is somewhat increased compared to the oligomer diradical. Thus, only 19% of the radical cation electron's spin density is left for the sum of the four remaining ring carbons and the four sulfur atoms.

We reported before[1] that radical cations occur also in (BBDT)Cl_2 or (BBDT)$(PF_6)_2$ solid salts owing to easy reduction of the dication with a typical concentration of about 1 per 40 molecules for the chloride salt. The ESR spectrum consists mainly of one broad line that is closer to Lorentzian than Gaussian in shape and some additional weaker structures more on the wings of the line. We derived

$$g = 2.0082 \pm 0.0006$$

from the zero-crossing of the differentiated line, and

$$(8.5 \pm 0.3)G_{pp} \leq \Delta B_{pp} \leq (10.5 \pm 0.3)G_{pp}$$

for different samples of the chloride salt and

$$g = 2.0088 \pm 0.0008$$

$$\Delta B_{pp} = (14.6 \pm 0.3)G_{pp}$$

for the PF_6 salt. The differentiated spectrum showed weak anomalies at field positions corresponding to the A_{zz} extrema of the frozen solutions. The g values are in keeping with the interpretation that these ESR spectra are dominated by the perpendicular components of the g tensor derived from the frozen solution experiment of **1b**.

3. Correlation of EPR Data with Extended Hückel Calculations. Molecular geometries for BBDT were optimized within the appropriate point group with a modified verison of GAMES.[12] Each optimization was performed using an STO-3G basis set and a gradient convergence tolerance of 0.01 mdyn/bohr. Spin densities for individual atoms were calculated using the extended Hückel method[13] with weighted H_{ij}'s.[14] Standard parameters were used for C, H, and N[13]. Sulfur parameters for the 3s orbital were H_{ii} (eV) = −20.00, $\xi_1 = 1.187$; for the 3p orbital, H_{ii} (eV) = −13.30, $\xi_1 = 1.817$. Sulfur d orbitals were excluded (see Table I).

Geometries for ^{2}BDT, ^{3}BBDT, and ^{2}BBDT were obtained as stated above[12] taking into account the proper oxidation state of the molecule. Bond distances were C–C, 1.40 Å; C–S, 1.77 Å; S–N, 1.76 Å; C–H, 1.09 Å. A reasonable geometry was assumed for the dimer diradical calculations with the N–N bond set to 1.5

(12) Dupuis, M.; Spangler, D.; Wendoloski, J. J. NRCC Software Catalog 1, Program No. QC01 (GAMES), Lawrence Berkeley Laboratorty, University of California, Berkeley, CA, 1980.
(13) Hoffmann, R.; Lipscomb, W. N. *J. Chem. Phys.* **1962**, *36*, 2179; **1962**, *37*, 2872. Hoffmann, R. *Ibid.* **1963**, *39*, 1397.
(14) Ammeter, J. H.; Bürgi, H. B.; Thibeault, J. C.; Hoffmann, R. *J. Am. Chem. Soc.* **1978**, *100*, 3686.

Table I. Charge Densities from EH Calculations[a]

atom	dimer diradical	monomer radical cation	^{3}BBDT	BDT
N	0.280/0.050[b]	0.205	0.165	0.298
S	0.170/0.056[b]	0.108	0.113	0.216
C_s[c]	0.042/0.058[b]	0.001	0.038	0.048
C_Y[d]	0.010	0.077	0.034	0.041
C_{H_2}[e]				0.046

[a] Quantities given are fraction of unpaired electron at a single atom site, normalized to one electron. [b] Corresponds to atoms near the central portion of the dimer diradical. [c] Corresponds to carbon atoms attached to sulfur atoms. [d] Corresponds to carbon atoms attached to Y (cf. structure **1**). [e] Corresponds to carbon atoms attached to H_2 in structure **2**.

Å. The nitrogen atoms were assumed to be similar to hydrazine in coordination with the lone pairs trans to each other.

For the monomer radical cation, we found in the calculations the largest spin densities in the two unsubstituted benzene positions (8%, atoms labeled Y in **1**), comparable with 10%, found experimentally. For the same type of atoms in the N–N bonded dimer diradical and **2**, we find the calculated values of 1 and 4%, respectively; experiment gave the values of 3 and 2% for these atoms. For the carbon atoms bearing H_2 in **2**, the experimental (2%) and calculated (5%) spin densities are in qualitative agreement. Furthermore, the calculations support our previous conclusion regarding the equivalency of all four protons in **2**.

As was observed experimentally, the spin density on the nitrogen atoms (terminal nitrogen atoms in the dimer) increases on going from the monomer radical cation to the dimer diradical. Nevertheless, the total density on both nitrogen atoms is larger for the monomer radical cation (41%) than the dimer diradical (33%), in keeping with the larger observed g value for the monomer radical cation, $\Delta g \sim (2.5 \pm 0.6) \times 10^{-4}$. Our calculations for the dimer also suggest an explanation for the absence of any resolved N splitting from the N–N bonded nitrogens because the calculated spin density for these nitrogens is markedly weaker than the calculated spin density for the terminal nitrogen atoms.

Extended Hückel calculations for the dimer show that the two HOMO's of the dimer diradical are almost degenerate ($\Delta E \sim$ 0.05 eV). This result is in strong contrast with the calculation results on an hypothetical geometry-optimized monomeric BBDT triplet diradical where a ΔE of 0.81 eV for these highest occupied levels was found. Hence, if any monomeric **1a** exists, it will be in a singlet state. Such a conclusion is supported by the absence of ESR spectral characteristics of a triplet state.

Experimental Section

The experimental conditions for the acquisition of the ESR spectra are mentioned in the sections above.

Unless otherwise stated, all preparations were carried out in an inert atmosphere (usually Ar). NMR spectra were recorded with a Varian EM-360, 60-MHz spectrometer, infrared spectra were obtained with a Perkin-Elmer Model 1300 spectrophotometer, and UV–vis spectra were obtained with a Perkin Elmer Model Lambda 5 spectrophotometer. Elemental analyses were performed by Spang Microanalysis and University of California microanalysis laboratory, Berkeley, CA.

Benzobisdithiazole Dichloride[1] (BBDTCl$_2$). A suspension of 500 mg (2.4 mmol) of 1,2,4,5-benzenetetrathiol in 50 mL of dry CCl_4 was cooled to −5 °C. Introduction of a brisk flow of chlorine quickly turned the reaction mixture yellow, then orange. Within 20 min (temperature kept <0 °C), a clear orange solution had formed. The excess chlorine was removed by flushing with argon and then the CCl_4 was removed under high vacuum (<0 °C). The resultant sulfenyl chloride (orange needles) was dissolved in 50 mL of dry CH_2Cl_2 and cooled to 3 °C. Then 0.65 mL (0.56 g, 4.9 mmol) of trimethylsilyl azide was added all at once. A deep red color quickly formed followed by gas evolution. The precipitated product made stirring difficult so an additional 10 mL of CH_2Cl_2 was added. The gas evolution had ceased within 2 h as the reaction mixture was allowed to warm to room temperature. After Schlenk filtering and copiously washing the product with CH_2Cl_2, it was vacuum dried overnight. A yield of 679 mg (93%) of hygroscopic, iridescent purple microcrystals was obtained.

IR (KBr) 3000 w, 1625 w, 1540 w, 1475 w, 1390 m, 1330 s, 1230 w, 1160 m, 1080 m, 1095 m, 1040 w, 862 m, 765 s, 695 m, 640 m, 545 s, 430 m, 385 m. Anal. Calcd for $C_6H_2ClN_2S_4H_3OCl$: C, 22.5; H, 1.50; Cl, 22.18; N, 8.75; S, 40.00. Found: C, 24.48; H, 1.06; Cl, 22.17; N, 8.29; S, 39.90; Si, 0.78.

Benzobisdithiazole Dihexafluorophosphate [BBDT(PF$_6$)$_2$]. A 0.50 M solution of $NOPF_6$ in dry CH_3CN was slowly added to 1 mmol of $BBDTCl_2$ with stirring. Initially, a dark red solution formed and a gas (NOCl–ppt AgCl with aqueous $AgNO_3$) was evolved. Upon addition of 2.0–2.5 mmol of $NOPF_6$ solution over ~30 min, virtually all the solid dissolved. Rapid high-vacuum evaporation of the CH_3CN produced a mass of yellow microcrystals embedded in an amorphous brown matrix. (Attempts to recrystallize this crude material from a variety of solvents were unsuccessful.) The crude material was triturated with 2.0 mL of a 2:1 v/v CH_2Cl_2/THF solution which dissolved essentially all of the brown material as well as some of the yellow microcrystals. The red supernatant solution (radical cation; λ_{max} 575 nm) was withdrawn by syringe and the remaining solid triturated an additional three times with 2.0 mL each of CH_2Cl_2. After vacuum drying 0.6 to 0.8 mmol (60–80%) of golden-yellow microcrystals were obtained.

IR (KCl) 3080 w, 1550 w, 1485 w, 1400 m, 1345 m, 1320 m, 1290 m, 1172 w, 1140 m, 1090 m, 1050 m, 970 m, 820 vs, 630 m, 550 s, 485 m, 430 m. When a solution of this salt in CH_3CN was treated with a slight excess of $Ph_4P^+Cl^-$, a precipiate identical in all respects with the above BBDT dichloride was obtained.

Benzobisdithiazolyl (BDDT). Solutions of the diradical were routinely prepared by suspending equal amounts of $BBDTCl_2$ and silver powder (~1 mmol each) in 250–500 mL of dry refluxing CH_2Cl_2. The refluxing suspension quickly turned a deep blue (λ_{max} 575 nm), reaching maximum intensity after refluxing overnight. The concentration of the filtered supernatant solution was approximately 1 mM. Prolonged refluxing did not provide a higher concentration. In addition, attempts to obtain higher concentrations by evaporating the millimolar solutions produced not more concentrated solutions but rather an iridescent precipitate which could be redissolved in additional CH_2Cl_2. The supernatant could be filtered off and fresh CH_2Cl_2 added to produce more diradical solution. This process could be repeated a number of times until >90% of the theoretical amount of diradical had been obtained. The millimolar blue diradical solutions when stored under N_2 in the freezer were stable for several weeks. Calcd M^+: 229.910 amu. Found: 229.913, with the expected P + 1 and P + 2 peaks due to four sulfur atoms.

While the diradical could be prepared electrolytically from BBDT(PF$_6$)$_2$ in CH_3CN, the quality of the resultant material, as evidenced by ESR spectroscopy, was not good. It was frequently contaminated with the radical cation. Particularly sharp ESR spectra of the diradical could be obtained by stirring equal amounts of silver powder and $BBDTCl_2$ in dry $CDCl_3$ for a few minutes. The resultant very dilute solutions were then thoroughly freeze–thaw degassed in the ESR tube.

Dideuteriobenzobisdithiazole Dichloride (BBDTCl$_2$-d_2). A sample of 3,6-dideuterio-1,2,4,5-tetrakis(methylthio)benzene was prepared by refluxing 500 mg (1.9 mmol) of 1,2,4,5-tetrakis(methylthio)benzene in 0.25 mmol of deuterioacetic acid with a few milligrams of zinc dust added to suppress formation of the radical cation. After 24 h of reflux, the solvent was evaporated; the residue was washed with water then taken up into ether, washed, and dried. Recrystallization of the crude material gave a first crop of 180 mg. Integration of the NMR signal due to the residual aromatic proton signal at 7.1 ppm vs. the SMe signal at 2.5 ppm indicated 85% deuteration. This material was then reduced with Na in liquid NH_3. After sublimation, 58 mg of the tetrathiol was obtained; 14 mg of the deuterated tetrathiol was then converted to 12 mg of BBDTCl$_2$-d_2 using the approach described above.

Acknowledgment. This work was supported by NSF Grant DMR 82-17924 from the Solid State Chemistry Program.